

# IOTLB-SC: An Accelerator-Independent Leakage Source in Modern Cloud Systems

Thore Tiemann  
*University of Lübeck*

Zane Weissman  
*Worcester Polytechnic Institute*

Thomas Eisenbarth  
*University of Lübeck*

Berk Sunar  
*Worcester Polytechnic Institute*

## Abstract

Recent research in micro-architectural attacks has uncovered a variety of vulnerabilities on shared compute devices like CPUs and GPUs which pose a substantial threat to cloud service providers and customers alike. Cloud service providers have therefore moved towards flexible systems that prioritize re-arrangeable hardware components that are not shared between users to minimize attack surfaces while retaining scalability.

In this work, we show that for the sake of system security it is necessary to consider not only the security of the processors and peripherals of a system but also the security of the subsystems that connect them. In particular, we investigate the side-channel leakage potential of the I/O translation look-aside buffer (IOTLB) used in I/O memory management units (IOMMUs) to cache address translations. To exploit the IOTLB, we design a hardware module deployed to an FPGA to help us perform precise timing measurements. For the first time, we prove that the IOTLB is the source of a timing-based side-channel leakage and use it to create two covert channels from CPU to peripheral and between peripherals. While the first channel easily achieves an error rate of only 30%, the latter proved to be very reliable as nearly no errors occur. We present a close look at web fingerprints collected through this side-channel, and we examine the I/O operation of a GPU-accelerated SQL database. We then discuss several methods to remedy the observed side-channel leakages, including application design techniques, peripheral layout within existing systems, and micro-architectural features that could harden future IOMMUs.

## 1 Introduction

Micro-architectural attacks like Spectre [22] and Melt-down [25] made headlines when they showed how side effects of simple operations could violate the most basic security assumptions promised by memory isolation systems. More subtly, timing side-channels have exploited microprocessor caches [6, 12, 27, 55] and translation look-aside buffers

(TLBs) [9] to gain information about what another user is doing with shared hardware without actually violating the principles of memory isolation. Recently, major cloud providers have shifted more and more virtualized computation resources off of CPUs, and onto peripherals like smart network interface cards (NICs), smart storage, FPGAs, and GPUs [2, 3, 7]. These peripherals provide general purpose or application- and hypervisor-specific acceleration for an increasingly diverse set of tasks, including networking, 3D rendering, machine learning, stock trading, and cryptography, can also come with their own side-channel vulnerabilities when shared by multiple users, like performance counter and cache side-channels on GPUs [8, 34], internal cache side-channels on FPGAs [54], and power side-channels on FPGAs [48, 52, 58] and modern non-volatile memories [21].

Robust systems for managing cloud tenant isolation on CPUs and peripheral devices alike have been proposed [44], and cloud providers like Amazon Web Services claim that the virtualized hardware components in their systems are isolated for security rather than shared [3]. The systems that connect peripheral components and CPUs have been targeted at the logical level by attacks exploiting misconfigured IOMMUs [32, 33] or spoofing the behavior of trusted peripherals [28].

This work exposes a vulnerability in a largely overlooked attack surface: the micro-architecture of the IOMMU itself. We prove the existence of a timing-based IOTLB side-channel vulnerability that leaks performance information in modern IOMMUs, discuss potential threat models, and provide guidance and best practices for hardware engineers, cloud service providers, and developers of cloud applications for protecting themselves, their clients, and their customers from IOTLB side-channel attacks.

## Contributions

- We analyze the threat posed by IOTLB timing side-channel attacks against peripherals, with a focus on cloud environments.

- We develop a platform-agnostic algorithm for finding IOTLB eviction sets.
- We use a custom FPGA hardware function to exploit the IOTLB timing side-channel and study the data collected in two scenarios:
  - A web browser in a virtual machine accessing various websites with a network card.
  - An SQL database acceleration library for a GPU performing various lookups.
- We demonstrate the *first* two IOTLB covert channels, including a peripheral-to-peripheral channel with a generic application as the sender and our custom FPGA function as the receiver.
- We propose countermeasures to be implemented in applications, cloud systems, and IOMMU implementations to counter the side-channel we identified.

## 2 Background

When multiple hardware resources share data, it is often desirable to have direct memory access (DMA) from one resource to another. But simply allowing any peripheral to read or write a host CPU’s memory, for example, would be disastrous for security, especially in virtualized environments with multiple users sharing the CPU. AMD’s AMD-Vi and Intel’s VT-d features (present on both companies’ performance desktop and server processors for the better part of a decade) allow for virtualized DMA with IOMMUs that dynamically map and translate virtual addresses used specifically by peripherals to access CPU memory. To speed up repeated access to the same memory location, IOMMUs often include translation look-aside buffers (TLBs, or IOTLBs when they are in IOMMUs) which cache recently translated I/O virtual addresses and their corresponding physical addresses to avoid the slow page-table walks otherwise required for translation. But, like CPU caches and TLBs, which perform a similar function for CPU memory accesses and address translations, IOTLBs introduce a timing-based side-channel vulnerability.

### 2.1 Caches and TLBs

A cache stores data for faster access. A translation look-aside buffer (TLB) is technically just another cache, though rather than caching the data or instructions stored at an address, it caches an address translation. However, throughout this paper we will refer to memory caches as simply “caches”. Intel’s documentation [18] and several works reverse-engineering cache architectures [17, 20, 27, 37] and TLB architectures [9] reveal that TLBs on modern Intel CPUs are organized very similarly to modern CPU memory caches. Modern TLBs and caches are typically organized into **sets** and **ways**. The number of ways is the number of entries each set can contain.

For TLBs, each virtual address is mapped to one set, but can occupy any way within that set. When a set is full, old entries may be evicted to make room for new ones. A set of addresses which reliably causes the eviction of all other entries in a set when accessed is called an **eviction set**. A minimal eviction set contains as many addresses as there are ways in the cache/TLB and therefore fills an entire cache set when accessed [53].

### 2.2 Side-Channel Attacks

At the time of this publication, timing side-channel attacks against the CPU’s cache are widely studied and well understood: researchers have crafted several variants [6, 12, 27, 55], used them as part of more complicated micro-architectural attacks [22, 25], and built defenses against them [11, 26, 56].

Timing side-channel attacks, whether mounted against a CPU cache or a TLB, involve timing an operation or operations to determine whether or not an entry is present. On modern computer systems, almost all memory accesses use virtual addressing (and therefore a TLB) as well as the caching subsystem, and therefore leave traces in these systems which may be usable in an attack.

Years of study on cache architectures and timing side-channel attacks have produced many cache side-channel strategies that work in different memory-sharing scenarios and have quite varied temporal and address resolutions. These are some of the most common and useful attack techniques:

**Flush+Reload** Flush+Reload (F+R) [55] has three steps: **1)** The attacker flushes the cache line that is to be monitored. After flushing this cache line, **2)** she waits for the victim to execute. Later, **3)** she reloads the flushed line and measures the reload latency. If the latency is low, the cache line was served from the cache hierarchy, so the cache line was accessed by the victim. If the access latency is high, the cache line was not cached, meaning that the victim did not use it. Flush+Flush (F+F) [12] is similar to F+R, but the third step is different: the attacker flushes the cache line again and measures the execution time of the flush instruction instead of the memory access. Orthogonal to F+R, if the attacker does not have access to an instruction to flush a cache line, she can instead evict the desired cache line by accessing cache lines that form an eviction set in an Evict+Reload (E+R) [24] attack. Eviction sets are described shortly. F+R, F+F, and E+R are limited to shared memory scenarios, where the victim and attacker share data or instructions, e. g. when memory de-duplication is enabled.

**Prime+Probe** Prime+Probe (P+P) gives the attacker less temporal resolution than the aforementioned methods since the attacker checks the status of the cache by probing a whole cache set rather than flushing or reloading a single line. However, this resolution is sufficient in many cases

[4, 24, 31, 37, 38, 47, 57]. P+P has three steps: **1)** The attacker primes the cache set under surveillance with dummy data by accessing a proper eviction set, **2)** she waits for the victim to execute, **3)** she accesses the eviction set again and measures the access latency (probing). If the latency is above a certain threshold, some parts of the eviction set were evicted by the victim process, meaning that the victim accessed cache lines belonging to the cache set under surveillance [27]. Unlike F+R, E+R, and F+F, P+P does not rely on shared memory.

### 2.3 Attacks on TLBs

In 1995, Silbert et al. remarked in a security analysis of Intel CPU architectures that "all 80x86 [now more commonly called x86] processors have a translation look-aside buffer (TLB) that . . . has potential for use as a covert timing channel" [51]. In 2013, Hund et al. demonstrated that a TLB timing side-channel on then-modern Intel Nehalem and Sandybridge CPUs could reveal if a page was mapped by the operating system even if the user doesn't have permission to access the page directly [17]. They demonstrated that this exploit could be used to identify the pages used by the kernel, even when the addresses of the pages were randomized (a common defense against side-channel attacks of many types). In 2017, Gras et al. crafted an attack that uses a cache side-channel to identify TLB evictions. This was a robust attack that can be mounted even from JavaScript to de-randomize kernel pages [10]. Gras et al.'s "TLBleed" in 2018 [9] showed that TLBs in modern Intel CPUs were vulnerable to timing side-channel attacks of the sort that are typically used on CPU memory caches, and can be used for similarly complex attacks: with the help of some machine learning, the TLB side-channels on Skylake, Broadwell, and Coffeelake CPUs can be used to recover a key from an Edward-curve cryptographic function.

### 2.4 PCIe

Peripheral Component Interconnect Express (PCIe) [40] is the backbone of modern desktop and server systems. While often referred to as a bus, PCIe uses a high-speed point-to-point topology with devices being connected to switches or directly to a root port via serial links. In this paper, we are concerned with a single-root topology where only one root complex is part of the PCIe network. The root complex manages the network and assigns all devices connected to the network a unique address depending on their location in the network. It also connects the PCIe network to the CPU and the main memory. Figure 1 shows the general architecture of PCIe for better visualization. On a PCIe network, all devices can send memory requests to each other and to the main memory. An IOMMU can be used to virtualize addresses used by PCIe device and to implement access restrictions. Additionally, the root port may define access rules for inter-device communi-

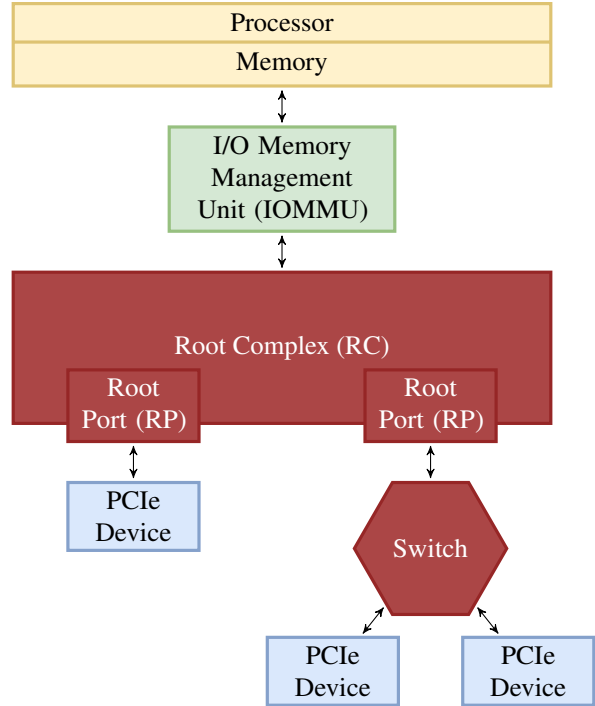


Figure 1: PCIe architecture, adapted from [41, 42]

tion and implement them in the PCIe switches, if supported by the switches.

### 2.5 IOMMUs

Input-Output Memory Management Units (IOMMUs) are located between PCIe devices and the main memory (cf. Figure 1). Usually, they are implemented as part of the root complex. Modern server systems feature one IOMMU per root port. Similar to MMUs in the CPU, IOMMUs provide address translation and protection for memory regions that are made accessible to PCIe devices [1, 19]. Address virtualization allows to isolate or virtualize such devices. Also, it allows 32-bit peripherals to use memory regions above 4 GB.

The translation process of the IOMMU works very similar to the process in a CPU's MMU. Modern IOMMUs map PCIe devices to IOMMU groups or domains. The operating system, hypervisor, or VMM maintains a page table with all address mappings per group/domain. The page table is organized in a tree structure. Its depth depends on the width of the I/Ovirtual addresses (IOVAs) supported by the IOMMU. Typical sizes are 39-, 48-, or 57-bit IOVAs. Address bits are translated in groups of 9 bits which results in page tables consisting of 3, 4, or 5 layers of tables, each storing 512 entries. For IOVAs referencing 4 KB pages, the 12 least significant address bits (page offset) remain untranslated. Accordingly, the 21/30 least significant bits of IOVAs for 2 MB/1 GB pages remain untranslated.

IOVAs are translated to physical addresses (PAs) by the IOMMU performing a page table walk. Since this is quite time consuming, modern IOMMUs feature a translation look-aside buffer called IOTLB. This cache is used to store translated IOVA→PA mappings and is shared by all devices managed by the IOMMU.

### 2.5.1 Attacks on IOMMUs

In the past, several attacks have been shown that circumvent the IOMMU to gain direct memory access or use the mis-configuration of the IOMMU to exploit device drivers through code injection or control-flow hijacking. However, the root cause always was a miss-configured IOMMU or a software vulnerability. We are not aware of any attacks that were made possible solely by the IOMMU hardware.

For example, a malicious peripheral can bypass the IOMMU by adding appropriate entries to the page table on startup before the IOMMU is activated by the BIOS [32, 33]. This is possible because PCIe devices learn their addresses early during the startup phase and can send valid requests before the BIOS finished the IOMMU configuration. Another way to escape the isolation through IOMMU address virtualization is possible for malicious peripherals supporting PCIe address translation services (ATS [41], also called “DeviceTLB”). Such devices can mark addresses as “translated” such that the IOMMU will forward them to the main memory without any further translation. This attack vector has been shown to be practical in [28] since operating systems tend to allow the ATS feature by default. After bypassing the IOMMU, a malicious device usually has unrestricted access to the main memory via direct memory access.

Malicious devices may also try to exploit vulnerabilities in the kernel or device drivers. This is often possible since the IOMMU address translation works only on a page granular level. However, I/O buffers are usually smaller than a full page which leads to other code or data being present in that page and being accessible by the device as well. [28, 29] show that such so called sub-page vulnerability may lead to secrets leaking to the device. If the device is allowed to write to the page, code injection or control-flow hijacking attacks become feasible. Since most device drivers run with root privileges, sub-page vulnerabilities easily lead to a full system compromise.

## 3 System Setup

We have access to three different system setups that we will investigate throughout this work. An overview of the setups is given in Table 1.

*a10l:* As our local setup we use a Dell PowerEdge R740 server with a Dell 0923K0 version A00 mainboard and two Intel Xeon Silver 4114 CPUs. Each CPU reports 4 PCIe root bridges with one DMA remapping (DMAR) hardware

unit per root port. All DMAR units report `ver 1:0 cap 8d2078c106f0466 ecap f020df`. The system contains a Realtek PCIe ethernet card at PCIe address `5e:00.0`. It is assigned to IOMMU group 37 which is managed by DMAR6 on NUMA node 0. The network interface controller (NIC) is passed-through to a virtual machine (VM) running on the server. An ethernet cable connects the NIC with one of the on-board NICs. Also, an NVIDIA Tesla T4 GPU is connected at PCIe address `86:00.0`. It is assigned to IOMMU group 49 managed by DMAR1 on NUMA node 1. An Intel Programmable Acceleration Card (PAC) with Intel Arria 10 GX FPGA is co-located with the NIC or the T4, depending on the experiment, by connecting it at PCIe address `5f:00.0` (DMAR6 on NUMA0) or connecting it at PCIe address `87:00.0` (DMAR1 on NUMA1). All other PCIe devices like the on-board ethernet adapters, memory controllers, etc. are connected to different DMAR units and therefore cannot interfere with our measurements. The system has Intel Acceleration Stack (IAS) 1.2 installed which contains OPAAE version 1.1.2-1. Running `fpgainfo` reports bitstream id `0x123000200000185` and bitstream version `1.2.3`. On the GPU we execute the GPU-accelerated database OmniSciDB<sup>1</sup> in version `5.10.1-20220125-f727c178bd`, which is the latest version at the time of writing. Additionally, CUDA version 11.4 and GPU driver version `470.57.02` are installed. The database consists of one table filled with the Meta Kaggle dataset<sup>2</sup>. We have root access to this machine.

*a10v:* The Intel vLab provides access to servers driven by an Intel S2600WFT version H48104-850 mainboard and two Intel Xeon Platinum 8180 CPUs. Each CPU reports 4 PCIe root bridges with one DMAR hardware unit per root port. All DMAR units report `ver 1:0 cap 8d2078c106f0466 ecap f020de`. Two PACs with Arria 10 GX FPGAs are connected via PCIe and reachable at addresses `18:00:0` (DMAR4, NUMA0) and `af:00:0` (DMAR2, NUMA1). All other PCIe devices are managed by other DMAR units. The servers use IAS 1.1 and OPAAE was installed on 01/01/2020 from the Git repository. Running `fpgainfo` reports bitstream id `0x113000200000177` and bitstream version `1.1.3`. There are four systems with this setup in the vLab. We operate these machines with user privileges only.

*s10v:* The Intel vLab provides access to servers driven by an Intel S2600WFT version H48104-851 mainboard and two Intel Xeon Platinum 8280 CPUs. Each CPU reports 4 PCIe root bridges with one DMAR hardware unit per root port. All DMAR units report `ver 1:0 cap 8d2078c106f0466 ecap f020de`. A Intel FPGA Programmable Acceleration Card D5005 is connected via PCIe and reachable at address `18:00:0` (IOMMU group 23, DMAR4, NUMA0). All other PCIe devices are managed by other DMAR units. The servers use IAS 2.0 and OPAAE was installed on 01/01/2020 from the Git repository. Running `fpgainfo` reports bitstream id

<sup>1</sup><https://docs.omnisci.com/overview/overview#omniscidb>

<sup>2</sup><https://www.kaggle.com/kaggle/meta-kaggle>

0x203000200000339 and bitstream version 2.0.3. There are 14 systems with this setup. We operate these machines with user privileges only.

## 4 Identifying IOTLB Side-Channels

To mount an IOTLB based side-channel attack, the latency difference between DMA accesses to addresses with cached translations and addresses without cached translation must be measurable for an attacker. Additionally, an attacker must be able to either flush specific translations from the IOTLB or construct eviction sets that are capable of evicting certain or all translations.

### 4.1 IOTLBs Cause Timing Behavior

During their PCIe performance benchmarking, Neugebauer et al. [35] proposed that an IOTLB miss results in a latency increase of 330 ns. Since the FPGAs in our systems are clocked at 200 MHz, the expected difference between fast and slow accesses is 66 clock cycles. Peglow’s [43] work matches our expectation. With disabled IOMMU, memory reads from any address in main memory are distributed around 160 and 185 cycles. When the system is configured to use the IOMMU, this distribution shifts to 225 and 270 cycles for addresses that are accessed for the first time. Access times for subsequent accesses are distributed similar to access times measured without IOMMU. So the measurable latency difference between accesses to addresses where the translation is present in or absent from the IOTLB lies between 65 and 85 clock cycles. We reproduced all values for the a101 system. On the vLab systems, the latency difference between first accesses and subsequent accesses lies in the expected range. However, we cannot disable the IOMMU on the vLab systems to check whether the latency difference disappears.

### 4.2 Constructing Eviction Sets

The IOMMU translates addresses for peripherals. Therefore, the CPU alone can only interact with the IOMMU in limited ways; we had to use a peripheral device to perform the experiments. For this purpose we used the Arria 10 GX, an FPGA accelerator on a PCIe expansion card with DMA capabilities. We designed a hardware function programmable from software to capture the required measurements.

We also had to develop a kernel module that allowed us to flush all entries from a given IOTLB. When it is loaded, the kernel module uses a variety of functions and structures from the Linux kernel source, including those found in `<linux/pci.h>`, `<linux/iommu.h>`, and `<linux/dmar.h>` to find a PCI device structure based on its vendor and device IDs, and from there find the device structure in kernel memory that controls the IOMMU that manages that PCIe device. That IOMMU device structure already contains a pointer to

a function for flushing the IOMMU, so that function merely needs to be called. The kernel module we developed uses a character file and `ioctl` as an interface by which user programs can call for the kernel module to flush the IOMMU. However, it takes root access to a system in order to load a kernel module, since the module must read and write kernel memory. Therefore, we could only test Algorithm 3 using the optional flush on our local system *a10l*.

#### 4.2.1 Hardware Design

We designed the hardware module `iotlb_pnp` that helps us perform memory accesses and time the access latency. `iotlb_pnp` can be programmed with up to 7 instructions. Currently, the design supports 5 instructions: `evset_prime`, `evset_probe`, `target_prime`, `target_probe`, and `wait`. Configuration and programming of the hardware module is performed via MMIO through OPAE. The prime instructions make the hardware module access a pre-configured address (target) or set of addresses (eviction set). Probe instructions behave in the same way as the prime instructions but additionally count clock cycles. When probing an eviction set, the module can be configured to either measure the overall execution time of the instruction or time each memory access individually. The eviction sets used during priming and probing can be configured independent from each other, as is the case for the target instructions. The wait instruction simply makes the hardware module do nothing for a configured number of clock cycles.

#### 4.2.2 Software

The software counterpart to the hardware module uses the OPAE C library to interact with the hardware design on the FPGA. This library allows us to control and observe the operation of the hardware module with memory-mapped I/O (MMIO) as well as — crucially for the work that this module must do — allocate shared pages of the system’s main memory that the FPGA as well as the CPU can read and write.

#### 4.2.3 Testing Eviction Sets on a Simple Side-Channel

Initially, we assumed that the IOTLB would be organized like a CPU TLB, with  $2^s$  sets where  $s$  is an integer, some small number of ways per set, and a set mapping algorithm wherein the lowest  $s$  bits of the page address select the set number or some other combination of various bits of the page address forms the set number that the page is associated with. This assumption was grounded in the reverse-engineering results presented in [9] and the fact that IOTLBs and TLBs basically cache the same type of data and would therefore be implemented in a similar way. Initial experiments showed that 128-address eviction sets reliably evicted any other single address, so we hypothesized that the IOTLB was organized

Table 1: Overview of the system setups used in this work

Name	CPU	#PCIe RP	#IOMMUs	FPGA	OPAE ver.	Bitstr. ver.
<i>a10l</i>	2 Xeon Silver 4114	4 per CPU	4 per CPU	Arria 10 PAC	1.1.2-1	1.2.3
<i>a10v</i>	2 Xeon Platinum 8180	4 per CPU	4 per CPU	Arria 10 PAC	2020-01-01	1.1.3
<i>s10v</i>	2 Xeon Platinum 8280	4 per CPU	4 per CPU	Stratix 10 PAC	2020-01-01	2.0.3

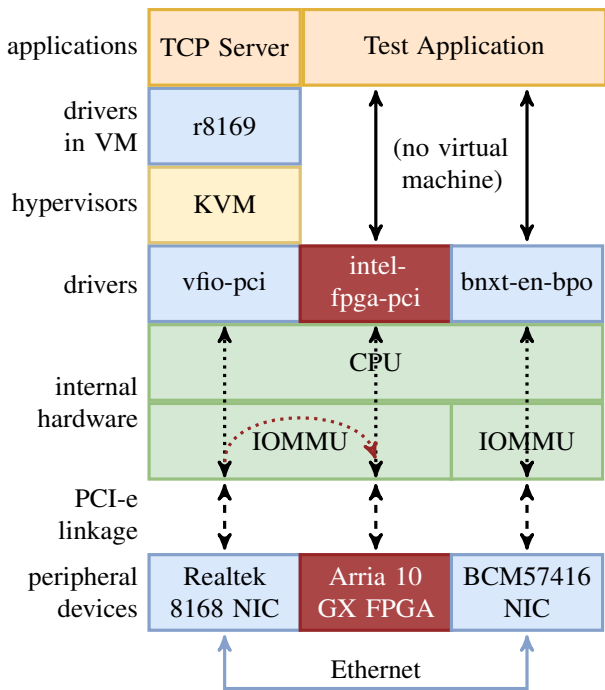


Figure 2: Stack diagram of the network card side-channel test. The Realtek 8168 network interface card (NIC) is "passed through" to a virtual machine with the VFIO driver. The test application exchanges packets with the TCP server in the virtual machine over the ethernet connection between the two network cards; meanwhile, the FPGA (connected to the same IOMMU as the VM's network card) probes the IOTLB for traces of network activity.

with 128 sets and 1 way. We tested this hypothesized eviction set architecture in a simple test scenario to verify that it would be usable for a Prime+Probe side-channel, and found unexpected results.

Figure 2 shows the hardware and software setup for this test. A virtual machine is configured with the IOMMU in a pass-through mode (Virtual Function I/O or VFIO) to allow a Realtek 8168 NIC direct access to the virtual environment, where it uses the standard r8168 drivers. The test application runs on bare metal, and uses the Broadcom BCM57416 NIC to exchange packets with the Realtek NIC over Ethernet. The test application also manages our Prime+Probe hardware on

Consistent Evictions in IOTLB During Network Test

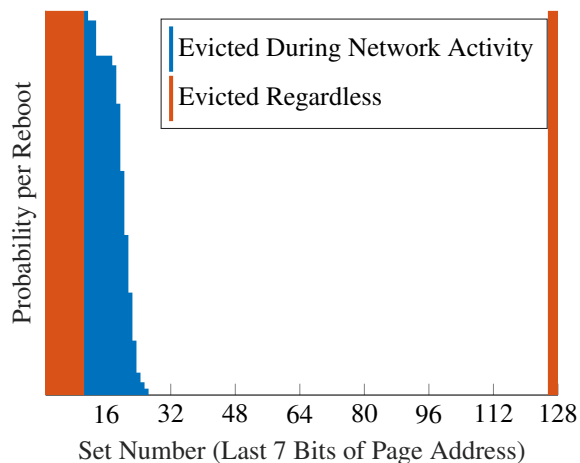


Figure 3: Behavior is consistent after a reboot of the virtual machine shown in 2, but inconsistent between reboots; this graph shows the likelihood that an IOTLB entry will be consistently read as evicted by a Prime+Probe after a reboot of the system. Entries marked in red are seen to be evicted whether or not there is network activity and do not vary between reboots; entries in blue are those that are evicted when there is network activity but not when there is no activity and vary significantly.

the Arria 10 GX FPGA and uses it to collect IOTLB side-channel traces while the network is active. The eviction sets used in the Prime+Probe tests are constructed under the assumption that the IOTLB contains 128 sets of 1 way each.

More evictions were detected in the probes of the Prime+Probe while the network was active, confirming that our eviction sets were measuring a side-channel leakage from the Realtek NIC. We also observed evidence of two unexpected behaviors of the IOTLB in the Prime+Probe data from this experiment that are visualized in Figure 3. First, the excess evictions caused by the network activity, shown in blue in the figure, varied substantially in the number of sets they occupied. Whenever the virtual machine was rebooted, the number of sets that would cause evictions in the probe during network activity appeared to be randomized, but there were always evictions in one set (set 11). After examining the network

Table 2: Notation used in algorithms

Symbol	Meaning
$A \leftarrow B$	$A$ gets the value of $B$
$A \leftarrow_{\in} B$	$A$ is chosen randomly from the set $B$
$A \leftarrow_{+} B$	$B$ is added to the set $A$
$A \leftarrow_{-} B$	$B$ is removed from the set $A$
$A \leftarrow_{/} B$	All elements in set $B$ are removed from $A$

**Algorithm 1:** evsetFinding(poolSize)

```

pool ← alloc(poolSize)
targets ← ∅
evsets ← ∅
while poolSize > 0 do
  target ←∈ pool // Sample random page
  pool ←- target
  if evsets do not evict target then
    targets ←+ target
    evsets ←+ constructEvset(target, pool)
    pool ←/ evsets

```

driver source code, we found that it allocates the transaction buffers used by the network card by calling a kernel function `dma_map_single` on startup, and we verified that by unloading and reloading the network driver, we could reproduce the randomizing effect of rebooting the virtual machine.

Second, we saw that sets 1-10 and 126-128 were always evicted in the probe, even absent any network activity or with the network drivers unloaded. This showed that our hypothesized 128-set eviction sets, while effective in evicting IOTLB entries, were actually bigger than necessary, since they were evicting their own members.

#### 4.2.4 A New Approach to Eviction Set Construction

We developed a novel and platform-independent algorithm for finding eviction sets with the help of our hardware module for any TLB or cache where the timing difference between a present entry and an evicted entry is known and measurable. Our algorithm is inspired by the Baseline Reduction Algorithm in [53]. The major difference is that, in contrast to [53], we do not know the expected size of an eviction set. We circumvent this drawback by using the grow-reduce approach presented in [27]. The inner workings of our algorithm are depicted in Algorithm 1. The program first allocates a pool of memory pages. It also manages two sets: The *targets* set is used to store the different target addresses used during eviction set construction. The *evsets* set stored all eviction sets constructed by the algorithm. After this initialization step, the algorithm picks a random target address from the pool and removes it from the pool. If *evsets* does not contain

**Algorithm 2:** constructEvset(target, pool)

```

evset ← ∅
contentions ← 0
// Grow
while contentions < 50 and |pool| > 0 do
  page ←∈ pool
  evset ←+ page
  pool ←- page
  if evicts(target, evset) then
    contentions ← contentions + 1
// Reduce
foreach page in evset do
  evset ←- page
  if not evicts(target, evset) then
    evset ←+ page
return evset

```

**Algorithm 3:** evicts(target, evset)

```

contention ← 0
for 0 ≤ i < 100 do
  flush IOTLB // optional
  target_prime()
  evset_prime()
  time ← target_probe()
  if time is greater than some threshold then
    contention ← contention + 1
return contention = 100

```

an eviction set for the target address yet, an eviction set is constructed. The target address and the new eviction set are added to their corresponding sets. All addresses in the newly constructed eviction set are then removed from the pool. This part will repeat until the pool does not contain any addresses anymore.

The construction of an eviction set for a fixed target address is given in Algorithm 2. It takes a target address and a pool of addresses as inputs. The eviction set is initialized as an empty set. During the "grow" step random addresses are chosen from the address pool and added to the eviction set until the eviction set contains enough addresses to evict the target. Obviously, the eviction set may contain unnecessary addresses at this point. This is why a reduction step follows. During this step, each address is tested for its necessity. If an address is not needed, it gets removed from the eviction set and gets put back in the address pool.

How to check whether an eviction set actually evicts a target is shown in Algorithm 3. The software uses the hardware module described previously to perform a prime and probe test. First, the FPGA accesses the target followed by an

access to each address in the given eviction set. Then, the target is accessed again and the access latency is measured. We define that an eviction set evicts a target if the latency of the second access to the target is above a certain threshold. We choose the threshold in the middle of the observed latency gap between fast and slow accesses observed on the different systems. Before each prime and probe test, we optionally cleared the IOTLB.

### 4.3 Experimental Results

We found that the optional flushing of the IOTLB has an impact on the size and reliability of the constructed eviction sets. Enabling IOTLB flushes in Algorithm 3 will make Algorithm 1 return a single eviction set containing 117 addresses on our local system. In rare cases, the algorithm constructs two sets with 117 addresses each. This can be circumvented by waiting 100 ns between the IOTLB flush and the `target_prime()` to make sure that the flush is finished before continuing with the next step. The success rate of such eviction sets is 100% for any target address we ever tested. Disabling the flushing step, however, yields more eviction sets (see Figure 4 (Ca) - (Cd)). If the order of accesses during the `evset_prime()` is static throughout one run of Algorithm 1, the resulting eviction sets contain 20 to 25 addresses each (Figure 4 (Sa), (Sc)). The average success rate is slightly below the average success rate of eviction sets constructed with randomized access order during `evset_prime()`. In turn, randomizing the access order yields on average slightly less (Figure 4 (Cb), (Cd)) but bigger sets (Figure 4 (Sb), (Sd)). The success rate of these sets, with or without randomized access order, evict a target with probabilities above 90%. This behavior is measurable on all of our three test systems which lets us conclude that the IOTLB architecture on all three systems is very similar if not identical.

## 5 Analysis of Side-Channel Leakages

We will now use the constructed eviction sets to further investigate the amount of leakage observable in the IOTLB. We focus on two applications that make use of co-located peripherals: accessing websites through a network card and running an in-memory SQL database on a graphics card.

### 5.1 Web Access Leakage

In Section 4.2.3 we showed that the operation of a network card leaves traces in the IOTLB. With that, we set out to explore a common target for side-channel attacks: web fingerprinting. In a web fingerprinting attack, an attacker collects side-channel data while accessing various websites in a controlled environment and uses those data to build a model. Attacks have been built using a wide variety of data sources on a variety of platforms, including network traffic [16, 39], cache

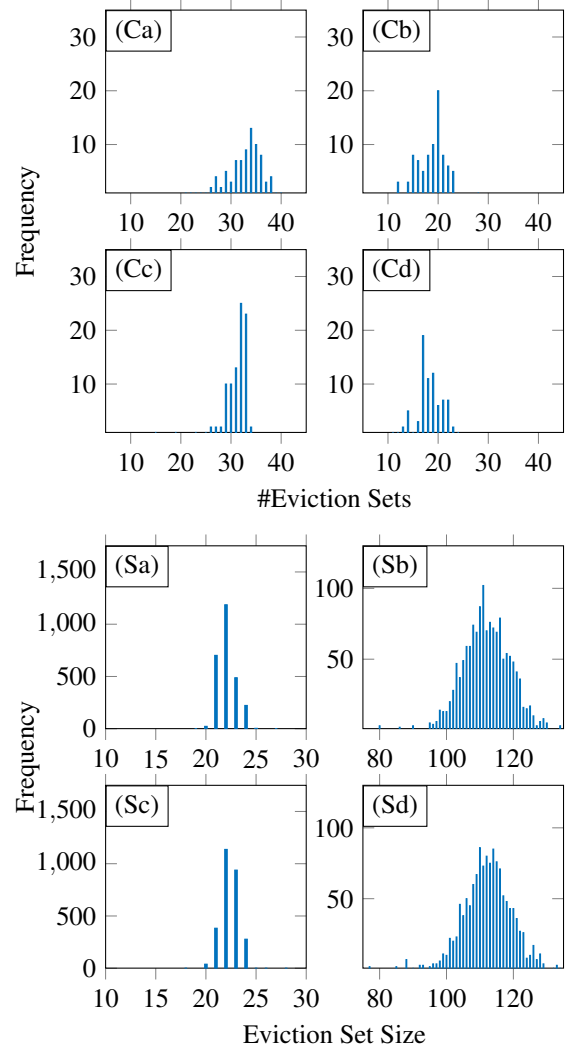


Figure 4: Number of eviction sets and the size of each constructed set needed to evict any target IOVA on the s10v system after running Algorithm 1 100 times each. During eviction set construction, randomization of the eviction set was turned off for measurements (a) and (c) and turned on for (b) and (d). For measurements (c) and (d), the algorithm waited 100 ns between each eviction test. For measurements (a) and (b) this was not the case.



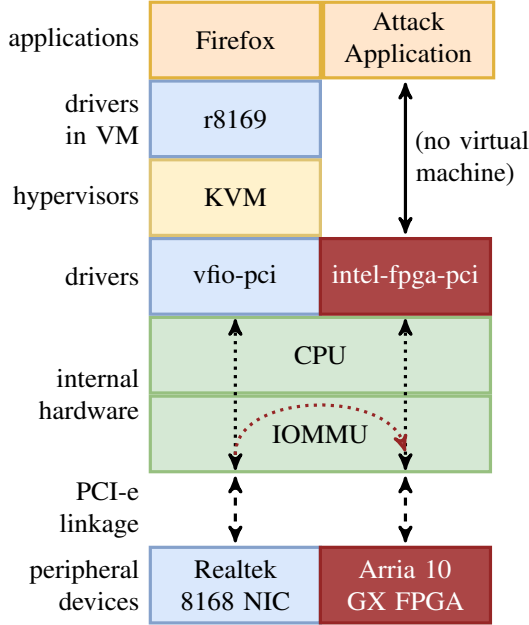


Figure 5: Stack diagram of the web access fingerprinting attack. The Firefox web browser runs on the VM and uses the network card with VFIO pass-through to access various websites. Meanwhile, the attacker periodically probes an IOTLB eviction set to collect fingerprints of network activity.

traces [14, 49, 50], and hardware performance events [13]. Then the attacker collects side-channel data from the victim and uses the model to predict the sites the victim was accessing.

We collected IOTLB Prime+Probe fingerprints while accessing a variety of websites from virtual machine using a PCIe network card co-located with the FPGA. As a browser, we used Firefox 88.0, the stable version available from the standard Ubuntu repositories at the time of data collection. We also collected side-channel data while the browser was inactive. Periodically, data collection was paused so the network card drivers could be reloaded. This triggers a reallocation of the relevant transmission buffers as described in Section 4.2.3; an attack on this network card to be practical it would have to work after any driver reset. IOTLB probing generates an extremely large amount of data, even when artificially slowed. We collected traces at 4,000 probes per second, or one probe every 250 microseconds. As a result, the data requires some pre-processing before a machine learning model can effectively learn the fingerprints of the sites.

First, each timing measurement is converted to a logical 1 or 0, 1 representing a probable eviction (a slow memory access), and 0 representing a faster access to an address that was not evicted. This binary signal is still quite information-dense, but a spectrogram reveals patterns in its frequency content that shift over time and visibly vary between websites. The low-

est frequency in the spectrogram was found to be extremely noisy compared to all others and was removed completely. The spectral data is then converted from amplitude to power and represented in decibels to tighten and normalize the distribution of data. Changes in the trace from one network driver reset to another must be accounted for in pre-processing as well. The mean of a random 70% of the idle signal (so that some variation from the remaining 30% could be observed) after a given reset of the network driver is subtracted from each other sample taken after that same reset. Because of the nature of the decibel scale, data points with zero power correspond to negative infinity decibels, which is inconvenient for batch comparisons of data, so all points below  $-100$  decibels were raised to  $-100$  decibels. Finally, all the samples were averaged; the interested reader may inspect the mean spectral data for each class after pre-processing in Appendix A.

Some distinguishing features of various sites are immediately clear in these spectrograms, like the relative absence of IOTLB activity when there is no network activity, a vertical band (broad spectrum signal across a short period of time) of activity early in the signal for all the sites followed by horizontal bands (consistent activity in certain frequency ranges across time). With a sophisticated machine learning model like those used in other web fingerprinting attacks [14, 46], these traces could likely be classified automatically.

## 5.2 GPU-accelerated SQL Database Leakage

We also investigated the amount of IOTLB leakage observable from the FPGA when it is co-located with a GPU that runs an SQL database. For our tests, we co-locate our FPGA with an NVIDIA Tesla T4 GPU and run the OmniSci SQL server on it. Figure 7 shows a stack diagram of the setup. The test application interacts with our hardware module on the FPGA to construct, prime and probe an eviction set for the IOTLB. Additionally, the application can issue SQL queries to the database which computes the result on the GPU.

The eviction set finding algorithm returns one set with 117 addresses because we flushed the IOTLB while constructing the eviction set. After constructing an eviction set for the IOTLB, the test app performs a prime the IOTLB. During the waiting phase, the app runs an SQL query on the GPU. We tested several queries of which some significantly differ in the size of the returned results. After the GPU computed the SQL result, the test app probes the eviction set.

Figure 6 (b) - (d) show probe measurements for queries returning no, one<sup>3</sup> and 409,600 rows of data from the database. During the measurement shown in Figure 6 (a), no query was executed on the GPU. The separate access times for each address in the eviction set are plotted along the x-axis. The y-axis shows the measured latency for this address. Clearly, the GPU leaves a footprint in the IOTLB when it computes an SQL query. However, it is not possible to spot a difference

<sup>3</sup>One row in our case contains 36 bytes of data.

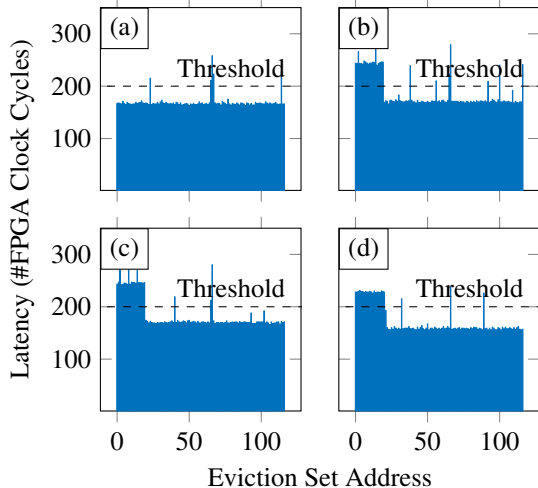


Figure 6: Measurements for the conducted experiments with the SQL database. During measurement (a), the test app did not run any query. The queries run in measurements (b) - (d) returned no, one and 409600 rows of data from the database. It is clearly visible that the SQL queries leave a footprint in the IOTLB.

between the three queries even if their results significantly differ in size.

Changing the test app to probe the eviction set while the SQL query executes on the GPU shows that the observable activity in the IOTLB is similar for all queries over time, besides the fact that queries with larger results produce longer traces as it takes longer to compute the result. Interestingly, the activity in the IOTLB happens towards the beginning of the query’s computation. At the time where the computed result is sent back to the CPU, there is no activity in the IOTLB.

This is easily explained by the way CUDA realizes the data transfer of the result from the GPU to the CPU: it uses MMIO<sup>4</sup> instead of DMA<sup>5</sup>. We verified the explanation by inspecting the PCIe performance counters with the PCM tools<sup>6</sup>. The performance counters showed an increased amount of MMIO read requests that in total match the size of the returned result.

Controlling an accelerator via MMIO rather than through DMA is a common usage model and limits the attack surface for IOTLB-based side-channel attacks dramatically because the CPU performs the address translation in the CPU’s MMU instead of the GPU translating addresses via the IOMMU. Obviously, MMIO leaves traces in the TLB of the CPU and might therefore not be the golden countermeasure against IOTLB side-channel attacks. Also, for very large databases that exceed the size of the GPU’s internal memory, leaking

DMA operations might be performed by the GPU to move data in and out of the GPU as needed.

## 6 Covert Channels

After identifying the IOTLB leakage and different ways to trigger and observe it, we will now use our knowledge to construct two covert channels to prove the practicability of the channel.

### 6.1 Covert Channel from CPU to Peripheral

The CPU is very limited in interacting with the IOTLB directly. Because the IOMMU translates addresses for peripherals only, memory accesses from the CPU do not interfere with the IOTLB. The only way for the CPU to interfere with the IOTLB is by changing page table entries or instructing the IOMMU to flush certain (or all) entries in the IOTLB.

Since a peripheral can distinguish IOTLB hits from misses, flushing the IOTLB allows the CPU to send information covertly to peripherals. A global IOTLB flush takes  $17\ \mu\text{s}$  on average. Flushing all entries from the IOTLB encodes a 1 and sleeping for  $17\ \mu\text{s}$  encodes a 0. As the receiver we use the hardware module described in Section 4.2.1. The hardware function is programmed to continuously probe a fixed target address. Whenever a probe reports a slow access, a 1 is received. Otherwise, the hardware receives a 0. We implement the covert channel in a trivial way without applying any encoding for error correction or synchronization. Because a memory access from the FPGA running at 200 MHz only takes around  $1\ \mu\text{s}$  we roughly synchronize the FPGA with the CPU by making the FPGA wait for a certain amount of cycles. We determined the number of cycles to wait by repeatedly sending a block of all-ones and increasing the number of wait cycles until the number of received zeros is minimal. We verified the received message by visual inspection. After this very rough synchronization step, we send a message of  $2^{16} - 1$  bits generated by a linear feedback-shift register to measure throughput and error rates. The result is given in Table 3. It turns out that this basic covert channel without further optimizations already achieves a throughput of around 15 kBit/s. The error rate is 30% which we assume can be improved significantly by applying error-correction and error-handling techniques as e. g. described in [30].

Because so far the covert channel only offers communication in one direction, we tried to improve the channel to offer bi-directional message transfer. To do so we checked the timing behavior of flushing the IOTLB. The `clflush` instruction on x86 CPUs has a data-dependent execution time [12]. In our case, a data-dependency of the flush time on IOTLB entries would allow us to construct the reverse covert channel. However, our experiments show no timing behavior of the flush that can be related to the usage of the IOTLB. Our

<sup>4</sup>The CPU initializes the data transfer.

<sup>5</sup>The peripheral initializes the data transfer.

<sup>6</sup><https://github.com/opcm/pcm>

Table 3: Throughput and error rate for the covert channels tested on the a10l system.

Channel	Throughput	Error rate	0-1-ratio
CPU → FPGA	15023 bps	30.09%	
GPU → FPGA	3.4 bps	0%	0% - 100%
GPU → FPGA	6.65 bps	0%	50% - 50%
GPU → FPGA	246.15 bps	0.1%	100% - 0%
GPU → FPGA	7.58 bps	0%	ASCII text

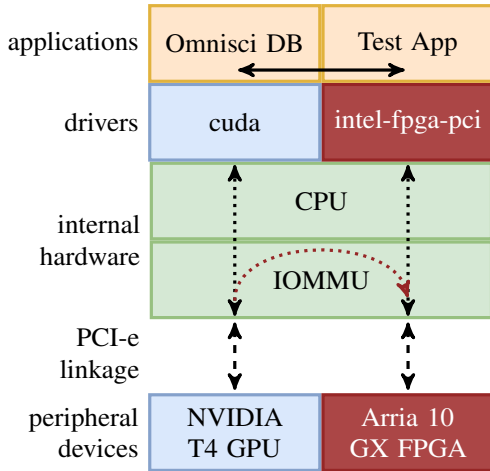


Figure 7: Stack diagram of the GPU accelerated SQL database covert channel and side-channel tests.

benchmarks show that an IOTLB flush takes around  $17\mu s$  independent of the FPGA performing memory accesses before or even during the flush. The timing is also independent from whether only addresses of a certain peripheral or all entries of the IOTLB are flushed.

The demonstrated covert channel was shown to be reliable without applying special synchronization, error-correction, or error-detection techniques. However, only peripherals can act as the receiver while the CPU is limited to the role of the sender. Also, with the standard IOMMU drivers in Linux, the sending process is required to run kernel-level code to perform IOTLB flushes. The channel might still be exploitable as a side-channel against device drivers that make extensive use of IOTLB flushes. For example, a driver developer may chose to include IOTLB flushes to remove traces of a peripheral’s activity for security; however, this might open a new side-channel if the timing of flushes reveals anything about the operation of an application using that peripheral.

## 6.2 Covert Channel between Peripherals

Another research question is whether two peripherals can use the IOTLB to construct a covert channel between each other.

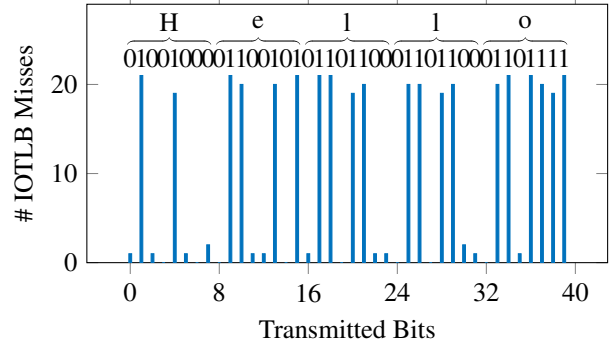


Figure 8: GPU to FPGA covert channel measurement. The GPU sends the message “Hello” in big endian format.

To answer this question, we co-locate the Arria 10 with the Tesla T4 again. Our goal is to use the footprint that an SQL query computed on the GPU leaves in the IOTLB to send information to the FPGA. Such a covert channel exists in a scenario where the sender uses a website that, depending on the actions performed on the website, runs SQL queries on a GPU-accelerated database. The sender can then exploit the website to send information to the co-located FPGA.

We prepare the server as shown in Figure 7. The sender encodes a one into running an SQL query and running no query encodes a zero. The receiver uses the hardware function on the FPGA to monitor the IOTLB using the Prime+Probe technique. During our experiments, we found that each SQL query evicts 18-20 entries of the receiver’s eviction set (cf. Figure 6 (b) - (d)). A plot of the number of IOTLB misses measured during message transmission is given in Figure 8. We found that basically no errors occur if sender and receiver are synchronized. The channels throughput highly depends on the number of one bits in the message. This is because the execution time of a single SQL query takes about 0.3 seconds. Table 3 shows more detailed measurements for different 0-1-ratios in the message that is transferred over the covert channel. Of course, a GPU application optimized for acting as a sender in this covert channel scenario would allow us to increase the bandwidth of the channel.

In our tests, the eviction set used by the FPGA was constructed with IOTLB flushes to work with eviction sets of optimal reliability. As mentioned before, IOTLB flushes require kernel privileges on commodity Linux systems. User-level receivers have to fall back to the less reliable eviction sets constructed without IOTLB flushes. It is expected to see a reliability degradation of the covert channel that is directly proportional to the reliability of the eviction set. Of course, this degradation can be circumvented by using error-correcting and error-detection mechanisms. This covert channel works between any two peripherals. Sender and receiver must be allowed to access pages in main memory. For the receiver,

the accessible buffer needs to be big enough to construct an eviction set. Additionally, the receiver needs a mechanism to measure the memory access latency. Peripherals that manage secrets and perform DMAs depending on the value of the secret must be aware that neighboring devices connected to the same IOMMU may be able to observe their access patterns. This is especially true for peripherals where the programming model assumes unified memory that abstracts separate physical memory locations like device and system memory away from the developer as in this case the leaking DMA may occur without the knowledge of the developer.

## 7 Countermeasures

Like many many micro-architectural attacks, there are a wide variety of defenses against IOTLB side-channels that can be implemented at nearly any level of a system. Hardware designs can be modified to allow for finer control of micro-architectural operations, system administrators and firmware developers can configure existing hardware in safer ways, and application developers can take steps to obfuscate leakage of security-critical functions.

**Isolation** IOTLB side-channels threaten the security of a device’s use of the IOMMU whenever a non-trusted device shares that IOMMU. However, most systems include multiple IOMMUs. In cases where multiple users who do not necessarily trust each other may use the same machine and have full and direct access to one or more PCIe peripherals in a virtual environment (as is now commonly the case with network interface cards, graphics cards, etc. on cloud platforms), ensuring that no two users (or no one user and the hypervisor) have access to peripherals on the same IOMMU hardware is sufficient to protect against IOTLB side-channel attacks. On Linux, information on a systems IOMMU devices and the PCIe devices that use them can be found in `/sys/class/iommu/` [45].

Typically, systems have several IOMMU devices, each of which is linked to a few PCIe endpoints, which may be internal PCIe devices or external devices plugged into PCIe slots on the motherboard. Devices cannot be reassigned to new IOMMUs, so ensuring full isolation may limit scaling capacity, particularly in cloud environments. For example, a cloud service provider could not use a motherboard with eight full-size, full-speed PCIe slots managed in pairs by four IOMMUs to provide eight fully isolated single-GPU cloud instances, even though eight GPUs fit in the PCIe slots of the system.

**Address Translation Services** If the IOMMU and the device to be isolated both support PCIe Address Translation Services (ATS) [41], then isolation is achievable by allowing the device to use ATS. ATS allows the device to maintain and

use a local on-device TLB for address translation. PCIe memory access request packages contain a “translated” bit that can be set by ATS supporting devices to inform the IOMMU that the requested address is a physical address and does not need to be translated by the IOMMU. If the OS/hypervisor/VMM allows ATS to be used by the device, the IOMMU forwards the memory requests without further translating the address. Therefore, using ATS to realize device-private IOTLBs is an easy way to isolate PCIe devices from each other.

However, allowing ATS for all devices in general is not advised. ATS allows a device to provide *any* physical address and mark it as “translated”. Malicious devices may exploit ATS for unrestricted memory access [28]. Therefore, ATS must only be allowed for trusted devices. Extra care has to be taken when configurable hardware like FPGAs that are re-programmable by tenants or graphics cards that can run arbitrary code come into play. In this case, allowing a tenant to use ATS with their own hardware or software would compromise the integrity of the entire host memory system. However, a non-user-reconfigurable region of an FPGA could use ATS without opening a direct vulnerability to any tenant with access to the FPGA, though of course then the security and integrity of the non-reconfigurable region must be trusted as any other ATS device.

**IOTLB Partitioning** A separation of the IOTLB between mutually untrusted tenants can also be achieved by IOTLB partitioning. If the IOTLB is set-associative, set partitioning can be done by the hypervisor directly in software by only allocating I/O virtual addresses belonging to certain sets to each tenant [56]. However, set-based partitioning may not work with peripherals that rely on the address space being contiguous. In this case, way-based partitioning is another option. But way-based partitioning needs to be supported by the IOMMU so that the hypervisor can map each address of a thread to a fixed number of ways like it is possible with Intel CAT [26, 36] for CPU-internal caches.

**Constant Time Code and Hardware** If code and hardware involved in data dependent computation perform all operations in constant time and with constant memory access patterns, then no information about the operations is leaked through the IOTLB. For cryptographic implementations this is a common technique. For database systems, constant memory access patterns and timings are not easily achieved. In some cases Private Information Retrieval (PIR) protocols [5, 23] can be a solution. However, modern PIR implementations<sup>7</sup> usually only support index queries. Recent attempts [15] to also support range queries may still leak information about the response size.

<sup>7</sup>e.g. <https://github.com/ReverseControl/MuchPIR>

**Reallocation of DMA Pages** Forcing a reallocation of pages that a device uses for DMA right before running a sensitive operation will confuse fingerprinting attacks by reshaping access patterns. However, timing variation may still leak some information about the operations. Reloading device drivers will typically be sufficient to reallocate all DMA buffers that a device uses. Alternatively, a driver itself could implement reallocation as needed.

**Disabling IOTLB Caching for Sensitive Pages** An IOMMU could be designed to support flagging a page translation as uncacheable, ensuring that it is never stored in the IOTLB. This would mean that the use of that page would never affect the IOTLB state, so it would be invisible to any side-channel attack. However, all accesses to that page would be as slow as IOTLB misses, increasing latency and likely reducing maximum throughput.

The choice to make a page translation uncacheable would have to be made at the application or hypervisor level. An application developer could identify pages that will be used for security-sensitive operations and mark them as uncacheable, or a cloud service administrator could mark all mappings of one virtual environment with access to a lower performance peripheral as uncacheable, removing its ability to use the IOTLB at all, while allowing another environment with access to a higher performance peripheral attached to the same IOMMU to securely and privately use the IOTLB for faster access speeds.

**Use MMIO** Typically, the CPU configures a peripheral by writing to its registers via memory mapped I/O (MMIO) where the peripheral's registers (and sometimes also memory) are mapped into the CPU's address space. While a peripheral can always initiate DMAs to read/write data from/to the main memory, MMIO communication always is initiated by the CPU. This implies that traffic to/from the peripheral caused by MMIO does not leave any traces in the IOTLB as the CPU is the one performing the address translation. And this translation is done by the CPU's MMU instead of the IOMMU. Therefore, data transfers via MMIO are not observable in the IOTLB. However, they may be observable in the MMU's TLB and potentially through any other buffer on the same physical CPU core and throughout the CPU cache hierarchy.

## 8 Conclusion

State-of-the-art cloud environments use direct memory access managed by IOMMUs to offer high speed, low latency and isolated memory access to an increasingly wide variety of peripherals. These peripherals support and accelerate all sorts of applications and virtual hardware functions, including those that perform secure operations or handle sensitive data. In this paper we demonstrated that the IOTLBs used by IOMMUs

on these current- and next-generation systems for managing PCIe peripherals are vulnerable to side-channel attacks. We designed a hardware module for an FPGA accelerator card and used it to construct eviction sets for the IOTLB. With the so found eviction sets, we analyzed the leakage potential of two common peripherals, namely a NIC and a GPU, for one possible use-case each. The results prove that the IOTLB can be used as a side-channel to spy on co-located devices. We highlight this fact by showing a very reliable covert channel from the GPU to the FPGA where we use the database application running on the GPU to encode messages into the GPU's system memory access patterns. We also suggest a variety of hardware and software countermeasures against these attacks. Many of these countermeasures fully eliminate the threat of IOTLB side-channels, but at the same time reduce the speed of peripherals or scalability of the systems that host them. Therefore, when designing or choosing hardware for large-scale, high-performance, secure services, IOTLB threats must be acknowledged and IOTLB isolation measures must be carefully considered for the specific needs of the system.

## Acknowledgments

Worcester Polytechnic Institute is located on the traditional land of the Nipmuc people.

This research received partial funding, hardware donations, and extremely useful advice from Intel and its employees. We would like to especially thank Alpa Trivedi, Sayak Ray, and Thomas Unterluggauer from Intel. This research was also partially funded by the German Research Foundation (DFG) grant 456967092 (SecFShare), and by National Science Foundation grants CNS-1814406, CNS-2026913 and CNS-1931639.

## References

- [1] Advanced Micro Devices Inc., 2485 Augustine Drive, Santa Clara, CA 95054, USA. *AMD I/O Virtualization Technology (IOMMU) Specification*, 3.06-pub edition, Apr 2021.
- [2] Alibaba Cloud ECS. Introducing the sixth generation of Alibaba Cloud's elastic compute service.
- [3] Amazon AWS. AWS Nitro System.
- [4] Gorka Irazoqui Apecechea, Thomas Eisenbarth, and Berk Sunar. S\$A: A shared cache attack that works across cores and defies VM sandboxing - and its application to AES. In *2015 IEEE Symposium on Security and Privacy, SP 2015, San Jose, CA, USA, May 17-21, 2015*, pages 591–604. IEEE Computer Society, 2015.

- [5] Benny Chor, Eyal Kushilevitz, Oded Goldreich, and Madhu Sudan. Private information retrieval. *J. ACM*, 45(6):965–981, 1998.
- [6] Craig Disselkoen, David Kohlbrenner, Leo Porter, and Dean Tullsen. Prime+Abort: A timer-free high-precision L3 cache attack using Intel TSX. In *26th USENIX Security Symposium (USENIX Security 17)*, pages 51–67, Vancouver, BC, Aug 2017. USENIX Association.
- [7] Daniel Firestone, Andrew Putnam, Sambrama Mundkur, Derek Chiou, Alireza Dabagh, Mike Andrewartha, Hari Angepat, Vivek Bhanu, Adrian M. Caulfield, Eric S. Chung, Harish Kumar Chandrappa, Somesh Chaturmohta, Matt Humphrey, Jack Lavier, Norman Lam, Fengfen Liu, Kalin Ovtcharov, Jitu Padhye, Gautham Popuri, Shachar Raindel, Tejas Sapre, Mark Shaw, Gabriel Silva, Madhan Sivakumar, Nisheeth Srivastava, Anshuman Verma, Qasim Zuhair, Deepak Bansal, Doug Burger, Kushagra Vaid, David A. Maltz, and Albert G. Greenberg. Azure Accelerated Networking: SmartNICs in the public cloud. In Sujata Banerjee and Srinivasan Seshan, editors, *15th USENIX Symposium on Networked Systems Design and Implementation, NSDI 2018, Renton, WA, USA, April 9-11, 2018*, pages 51–66. USENIX Association, 2018.
- [8] Pietro Frigo, Cristiano Giuffrida, Herbert Bos, and Kaveh Razavi. Grand pwning unit: Accelerating microarchitectural attacks with the GPU. In *2018 IEEE Symposium on Security and Privacy, SP 2018, Proceedings, 21-23 May 2018, San Francisco, California, USA*, pages 195–210. IEEE Computer Society, 2018.
- [9] Ben Gras, Kaveh Razavi, Herbert Bos, and Cristiano Giuffrida. Translation Leak-aside Buffer: Defeating cache side-channel protections with TLB attacks. In *27th USENIX Security Symposium (USENIX Security 18)*, pages 955–972, Baltimore, MD, Aug 2018. USENIX Association.
- [10] Ben Gras, Kaveh Razavi, Erik Bosman, Herbert Bos, and Cristiano Giuffrida. ASLR on the line: Practical cache attacks on the MMU. In *24th Annual Network and Distributed System Security Symposium, NDSS 2017, San Diego, California, USA, February 26 - March 1, 2017*. The Internet Society, 2017.
- [11] Daniel Gruss, Julian Lettner, Felix Schuster, Olya Ohri-menko, Istvan Haller, and Manuel Costa. Strong and efficient cache side-channel protection using hardware transactional memory. In *26th USENIX Security Symposium (USENIX Security 17)*, pages 217–233, Vancouver, BC, Aug 2017. USENIX Association.
- [12] Daniel Gruss, Clémentine Maurice, Klaus Wagner, and Stefan Mangard. Flush+Flush: A fast and stealthy cache attack. In Juan Caballero, Urko Zurutuza, and Ricardo J. Rodríguez, editors, *Detection of Intrusions and Malware, and Vulnerability Assessment - 13th International Conference, DIMVA 2016, San Sebastián, Spain, July 7-8, 2016, Proceedings*, volume 9721 of *Lecture Notes in Computer Science*, pages 279–299. Springer, 2016.
- [13] Berk Gülmezoğlu, Andreas Zankl, Thomas Eisenbarth, and Berk Sunar. PerfWeb: How to Violate Web Privacy with Hardware Performance Events. In Simon N. Foley, Dieter Gollmann, and Einar Snekkenes, editors, *Computer Security – ESORICS 2017*, pages 80–97, Cham, 2017. Springer International Publishing.
- [14] Berk Gülmezoglu, Andreas Zankl, Caner Tol, Saad Islam, Thomas Eisenbarth, and Berk Sunar. Undermining user privacy on mobile devices using AI. *CoRR*, abs/1811.11218, 2018.
- [15] Junichiro Hayata, Jacob C. N. Schuldt, Goichiro Hanaoka, and Kanta Matsuura. On private information retrieval supporting range queries. In Liqun Chen, Ninghui Li, Kaitai Liang, and Steve A. Schneider, editors, *Computer Security - ESORICS 2020 - 25th European Symposium on Research in Computer Security, ESORICS 2020, Guildford, UK, September 14-18, 2020, Proceedings, Part II*, volume 12309 of *Lecture Notes in Computer Science*, pages 674–694. Springer, 2020.
- [16] Jamie Hayes and George Danezis. k-fingerprinting: A robust scalable website fingerprinting technique. In *25th USENIX Security Symposium (USENIX Security 16)*, pages 1187–1203, Austin, TX, August 2016. USENIX Association.
- [17] Ralf Hund, Carsten Willems, and Thorsten Holz. Practical timing side channel attacks against kernel space ASLR. In *2013 IEEE Symposium on Security and Privacy, SP 2013, Berkeley, CA, USA, May 19-22, 2013*, pages 191–205. IEEE Computer Society, 2013.
- [18] Intel Corporation, 2200 Mission College Blvd., Santa Clara, CA 95052, USA. *Intel 64 and IA-32 Architectures Optimization Reference Manual*, Jun 2016.
- [19] Intel Corporation, 2200 Mission College Blvd., Santa Clara, CA 95052, USA. *Intel Virtualization Technology for Directed I/O – Architecture Specification*, 3.1 edition, Jun 2019.
- [20] Gorka Irazoqui, Thomas Eisenbarth, and Berk Sunar. Systematic reverse engineering of cache slice selection in Intel processors. In *2015 Euromicro Conference on Digital System Design, DSD 2015, Madeira, Portugal, August 26-28, 2015*, pages 629–636. IEEE Computer Society, 2015.

- [21] Mohammad Nasim Imtiaz Khan, Shivam Bhasin, Bo Liu, Alex Yuan, Anupam Chattopadhyay, and Swaroop Ghosh. Comprehensive study of side-channel attack on emerging non-volatile memories. *Journal of Low Power Electronics and Applications*, 11(4), 2021.
- [22] Paul Kocher, Jann Horn, Anders Fogh, Daniel Genkin, Daniel Gruss, Werner Haas, Mike Hamburg, Moritz Lipp, Stefan Mangard, Thomas Prescher, Michael Schwarz, and Yuval Yarom. Spectre Attacks: Exploiting speculative execution. In *2019 IEEE Symposium on Security and Privacy, SP 2019, San Francisco, CA, USA, May 19-23, 2019*, pages 1–19. IEEE, 2019.
- [23] Eyal Kushilevitz and Rafail Ostrovsky. Replication is NOT needed: SINGLE database, computationally-private information retrieval. In *38th Annual Symposium on Foundations of Computer Science, FOCS '97, Miami Beach, Florida, USA, October 19-22, 1997*, pages 364–373. IEEE Computer Society, 1997.
- [24] Moritz Lipp, Daniel Gruss, Raphael Spreitzer, Clémentine Maurice, and Stefan Mangard. ARMageddon: Cache attacks on mobile devices. In *25th USENIX Security Symposium (USENIX Security 16)*, pages 549–564, Austin, TX, Aug 2016. USENIX Association.
- [25] Moritz Lipp, Michael Schwarz, Daniel Gruss, Thomas Prescher, Werner Haas, Anders Fogh, Jann Horn, Stefan Mangard, Paul Kocher, Daniel Genkin, Yuval Yarom, and Mike Hamburg. Meltdown: Reading kernel memory from user space. In *27th USENIX Security Symposium (USENIX Security 18)*, pages 973–990, Baltimore, MD, Aug 2018. USENIX Association.
- [26] Fangfei Liu, Qian Ge, Yuval Yarom, Frank McKeen, Carlos V. Rozas, Gernot Heiser, and Ruby B. Lee. CATalyst: Defeating last-level cache side channel attacks in cloud computing. In *2016 IEEE International Symposium on High Performance Computer Architecture, HPCA 2016, Barcelona, Spain, March 12-16, 2016*, pages 406–418. IEEE Computer Society, 2016.
- [27] Fangfei Liu, Yuval Yarom, Qian Ge, Gernot Heiser, and Ruby B. Lee. Last-level cache side-channel attacks are practical. In *2015 IEEE Symposium on Security and Privacy, SP 2015, San Jose, CA, USA, May 17-21, 2015*, pages 605–622. IEEE Computer Society, 2015.
- [28] A. Theodore Marketos, Colin Rothwell, Brett F. Gutstein, Allison Pearce, Peter G. Neumann, Simon W. Moore, and Robert N. M. Watson. Thunderclap: Exploring vulnerabilities in operating system IOMMU protection via DMA from untrustworthy peripherals. In *26th Annual Network and Distributed System Security Symposium, NDSS 2019, San Diego, California, USA, February 24-27, 2019*. The Internet Society, 2019.
- [29] Alex Markuze, Shay Vargaftik, Gil Kupfer, Boris Pismany, Nadav Amit, Adam Morrison, and Dan Tsafir. Characterizing, exploiting, and detecting DMA code injection vulnerabilities in the presence of an IOMMU. In Antonio Barbalace, Pramod Bhatotia, Lorenzo Alvisi, and Cristian Cadar, editors, *EuroSys '21: Sixteenth European Conference on Computer Systems, Online Event, United Kingdom, April 26-28, 2021*, pages 395–409. ACM, 2021.
- [30] Clémentine Maurice, Manuel Weber, Michael Schwarz, Lukas Giner, Daniel Gruss, Carlo Alberto Boano, Stefan Mangard, and Kay Römer. Hello from the other side: SSH over robust cache covert channels in the cloud. In *24th Annual Network and Distributed System Security Symposium, NDSS 2017, San Diego, California, USA, February 26 - March 1, 2017*. The Internet Society, 2017.
- [31] Ahmad Moghimi, Gorka Irazoqui, and Thomas Eisenbarth. CacheZoom: How SGX amplifies the power of cache attacks. In Wieland Fischer and Naofumi Homma, editors, *Cryptographic Hardware and Embedded Systems - CHES 2017 - 19th International Conference, Taipei, Taiwan, September 25-28, 2017, Proceedings*, volume 10529 of *Lecture Notes in Computer Science*, pages 69–90. Springer, 2017.
- [32] Benoît Morgan, Eric Alata, Vincent Nicomette, and Mohamed Kaâniche. Bypassing IOMMU protection against I/O attacks. In *2016 Seventh Latin-American Symposium on Dependable Computing, LADC 2016, Cali, Colombia, October 19-21, 2016*, pages 145–150. IEEE Computer Society, 2016.
- [33] Benoît Morgan, Eric Alata, Vincent Nicomette, and Mohamed Kaâniche. IOMMU protection against I/O attacks: A vulnerability and a proof of concept. *J. Braz. Comput. Soc.*, 24(1):2:1–2:11, 2018.
- [34] Hoda Naghibijouybari, Ajaya Neupane, Zhiyun Qian, and Nael B. Abu-Ghazaleh. Side channel attacks on GPUs. *IEEE Trans. Dependable Secur. Comput.*, 18(4):1950–1961, 2021.
- [35] Rolf Neugebauer, Gianni Antichi, José Fernando Zazo, Yury Audzevich, Sergio López-Buedo, and Andrew W. Moore. Understanding PCIe performance for end host networking. In Sergey Gorinsky and János Tapolcai, editors, *Proceedings of the 2018 Conference of the ACM Special Interest Group on Data Communication, SIGCOMM 2018, Budapest, Hungary, August 20-25, 2018*, pages 327–341. ACM, 2018.
- [36] Khang T. Nguyen. Usage models for Cache Allocation Technology in the Intel Xeon Processor E5 v4 family, 2016.

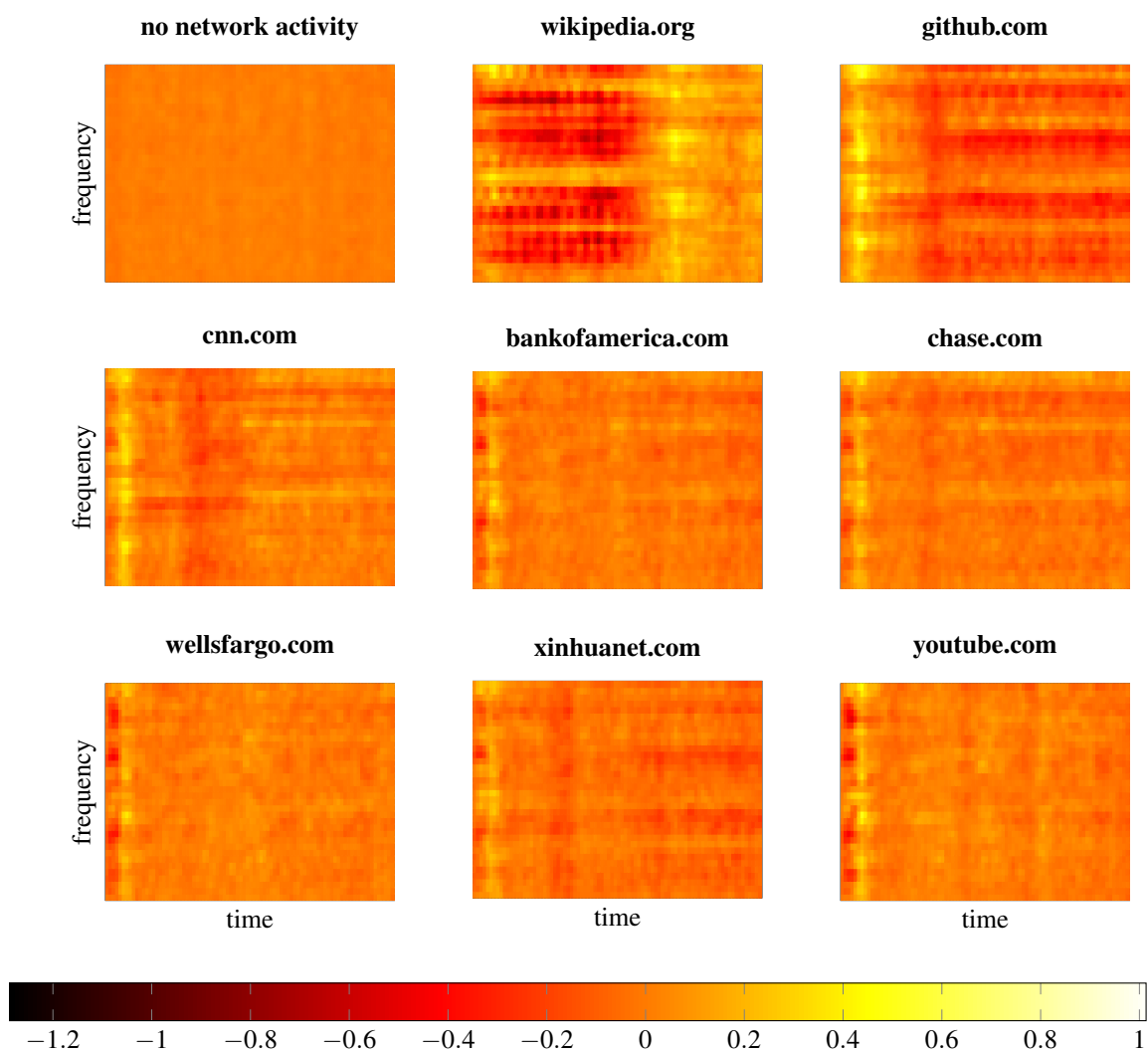
- [37] Yossef Oren, Vasileios P. Kemerlis, Simha Sethumadhavan, and Angelos D. Keromytis. The Spy in the Sandbox: Practical cache attacks in JavaScript and their implications. In Indrajit Ray, Ninghui Li, and Christopher Kruegel, editors, *Proceedings of the 22nd ACM SIGSAC Conference on Computer and Communications Security, Denver, CO, USA, October 12-16, 2015*, pages 1406–1418. ACM, 2015.
- [38] Dag Arne Osvik, Adi Shamir, and Eran Tromer. Cache attacks and countermeasures: The case of AES. In David Pointcheval, editor, *Topics in Cryptology - CT-RSA 2006, The Cryptographers' Track at the RSA Conference 2006, San Jose, CA, USA, February 13-17, 2006, Proceedings*, volume 3860 of *Lecture Notes in Computer Science*, pages 1–20. Springer, 2006.
- [39] Andriy Panchenko, Fabian Lanze, Jan Pennekamp, Thomas Engel, Andreas Zinnen, Martin Henze, and Klaus Wehrle. Website fingerprinting at internet scale. In *23rd Annual Network and Distributed System Security Symposium, NDSS 2016, San Diego, California, USA, February 21-24, 2016*. The Internet Society, 2016.
- [40] PCI-SIG, 3855 SW 153rd Drive, Beaverton, OR 97003, USA. *PCI Express Base Specification*, Dec 2006. Rev. 2.0.
- [41] PCI-SIG, 3855 SW 153rd Drive, Beaverton, OR 97003, USA. *Address Translation Services*, Jan 2009. Rev. 1.1.
- [42] PCI-SIG, 3855 SW 153rd Drive, Beaverton, OR 97003, USA. *Single Root I/O Virtualization and Sharing Specification*, Jan 2010. Rev. 1.1.
- [43] Christoph Peglow. Security analysis of hybrid Intel CPU/FPGA platforms using IOMMUs against I/O attacks. Master's thesis, University of Lübeck, Ratzeburger Allee 160, 23562 Lübeck, Germany, Jul 2020.
- [44] Kaveh Razavi and Animesh Trivedi. Stratus: Clouds with microarchitectural resource management. In Amar Phanishayee and Ryan Stutsman, editors, *12th USENIX Workshop on Hot Topics in Cloud Computing, HotCloud 2020, July 13-14, 2020*. USENIX Association, 2020.
- [45] RedHat, Inc. `/sys/class/iommu/<iommu>/devices/`, Jun 2014.
- [46] Vera Rimmer, Davy Preuveneers, Marc Juárez, Tom van Goethem, and Wouter Joosen. Automated feature extraction for website fingerprinting through deep learning. *CoRR*, abs/1708.06376, 2017.
- [47] Thomas Ristenpart, Eran Tromer, Hovav Shacham, and Stefan Savage. Hey, you, get off of my cloud: Exploring information leakage in third-party compute clouds. In Ehab Al-Shaer, Somesh Jha, and Angelos D. Keromytis, editors, *Proceedings of the 2009 ACM Conference on Computer and Communications Security, CCS 2009, Chicago, Illinois, USA, November 9-13, 2009*, pages 199–212. ACM, 2009.
- [48] Falk Schellenberg, Dennis R. E. Gnad, Amir Moradi, and Mehdi Baradaran Tahoori. An inside job: Remote power analysis attacks on fpgas. In Jan Madsen and Ayse K. Coskun, editors, *2018 Design, Automation & Test in Europe Conference & Exhibition, DATE 2018, Dresden, Germany, March 20-23, 2018*, pages 1111–1116. IEEE, 2018.
- [49] Michael Schwarz, Clémentine Maurice, Daniel Gruss, and Stefan Mangard. Fantastic timers and where to find them: High-resolution microarchitectural attacks in JavaScript. In Aggelos Kiayias, editor, *Financial Cryptography and Data Security*, pages 247–267, Cham, 2017. Springer International Publishing.
- [50] Anatoly Shusterman, Lachlan Kang, Yarden Haskal, Yosef Meltser, Prateek Mittal, Yossi Oren, and Yuval Yarom. Robust website fingerprinting through the cache occupancy channel. In *28th USENIX Security Symposium (USENIX Security 19)*, pages 639–656, Santa Clara, CA, August 2019. USENIX Association.
- [51] Olin Sibert, Phillip A. Porras, and Robert Lindell. The Intel 80x86 processor architecture: Pitfalls for secure systems. In *Proceedings of the 1995 IEEE Symposium on Security and Privacy, Oakland, California, USA, May 8-10, 1995*, pages 211–222. IEEE Computer Society, 1995.
- [52] Shanquan Tian, Shayan Moini, Adam Wolnikowski, Daniel E. Holcomb, Russell Tessier, and Jakub Szefer. Remote power attacks on the versatile tensor accelerator in multi-tenant FPGAs. In *29th IEEE Annual International Symposium on Field-Programmable Custom Computing Machines, FCCM 2021, Orlando, FL, USA, May 9-12, 2021*, pages 242–246. IEEE, 2021.
- [53] Pepe Vila, Boris Köpf, and José F. Morales. Theory and practice of finding eviction sets. In *2019 IEEE Symposium on Security and Privacy, SP 2019, San Francisco, CA, USA, May 19-23, 2019*, pages 39–54. IEEE, 2019.
- [54] Zane Weissman, Thore Tiemann, Daniel Moghimi, Evan Custodio, Thomas Eisenbarth, and Berk Sunar. JackHammer: Efficient rowhammer on heterogeneous FPGA-CPU platforms. *IACR Trans. Cryptogr. Hardw. Embed. Syst.*, 2020(3):169–195, 2020.
- [55] Yuval Yarom and Katrina Falkner. FLUSH+RELOAD: A high resolution, low noise, L3 cache side-channel attack. In *23rd USENIX Security Symposium (USENIX*



*Security 14*), pages 719–732, San Diego, CA, Aug 2014. USENIX Association.

- [56] Ying Ye, Richard West, Zhuoqun Cheng, and Ye Li. COLORIS: A dynamic cache partitioning system using page coloring. In José Nelson Amaral and Josep Torrellas, editors, *International Conference on Parallel Architectures and Compilation, PACT '14, Edmonton, AB, Canada, August 24-27, 2014*, pages 381–392. ACM, 2014.
- [57] Yinqian Zhang, Ari Juels, Michael K. Reiter, and Thomas Ristenpart. Cross-VM side channels and their use to extract private keys. In Ting Yu, George Danezis, and Virgil D. Gligor, editors, *The ACM Conference on Computer and Communications Security, CCS'12, Raleigh, NC, USA, October 16-18, 2012*, pages 305–316. ACM, 2012.
- [58] Mark Zhao and G. Edward Suh. FPGA-based remote power side-channel attacks. In *2018 IEEE Symposium on Security and Privacy, SP 2018, Proceedings, 21-23 May 2018, San Francisco, California, USA*, pages 229–244. IEEE Computer Society, 2018.

## A Mean Spectral Data Per Site



Mean of all training observations for each class in the model, after all pre-processing.